

Development 139, 4321-4329 (2012) doi:10.1242/dev.081869
 © 2012. Published by The Company of Biologists Ltd

SUMO1-activating enzyme subunit 1 is essential for the survival of hematopoietic stem/progenitor cells in zebrafish

Xiuling Li¹, Yahui Lan¹, Jin Xu¹, Wenqing Zhang^{2,*} and Zilong Wen^{1,*}

SUMMARY

In vertebrates, establishment of the hematopoietic stem/progenitor cell (HSPC) pool involves mobilization of these cells in successive developmental hematopoietic niches. In zebrafish, HSPCs originate from the ventral wall of the dorsal aorta (VDA), the equivalent of the mammalian aorta-gonad-mesonephros (AGM). The HSPCs subsequently migrate to the caudal hematopoietic tissue (CHT) for transitory expansion and differentiation during the larval stage, and they finally colonize the kidney, where hematopoiesis takes place in adult fish. Here, we report the isolation and characterization of a zebrafish mutant, *tango*^{hkz5}, which shows defects of definitive hematopoiesis. In *tango*^{hkz5} mutants, HSPCs initiate normally in the AGM and subsequently colonize the CHT. However, definitive hematopoiesis is not sustained in the CHT owing to accelerated apoptosis and diminished proliferation of HSPCs. Positional cloning reveals that *tango*^{hkz5} encodes SUMO1-activating enzyme subunit 1 (Sae1). A chimera generation experiment and biochemistry analysis reveal that *sae1* is cell-autonomously required for definitive hematopoiesis and that the *tango*^{hkz5} mutation produces a truncated Sae1 protein (Δ Sae1), resulting in systemic reduction of sumoylation. Our findings demonstrate that *sae1* is essential for the maintenance of HSPCs during fetal hematopoiesis in zebrafish.

KEY WORDS: Zebrafish, Hematopoiesis, SUMO-activating enzyme subunit 1

INTRODUCTION

In vertebrates, hematopoiesis shows two successive waves of development, which are known as primitive and definitive hematopoiesis. Primitive hematopoiesis produces myeloid and erythroid cells during the embryonic period (Haar and Ackerman, 1971; Takahashi et al., 1989). This transitory primitive hematopoiesis is subsequently replaced by a definitive hematopoietic program that gives rise to all blood cell lineages (erythroid, myeloid and lymphoid) during fetal and adult life (Galloway and Zon, 2003). The constant supply of fresh blood cells by definitive hematopoiesis relies on establishment of hematopoietic stem/progenitor cells (HSPCs), which have self-renewal capacity and can undergo differentiation into all lineages of mature blood cells (Cumano and Godin, 2007). In mice, HSPCs originate at embryonic day (E) 10.5 in the aorta-gonad-mesonephros (AGM) (Medvinsky and Dzierzak, 1996) and are found in the yolk sac and placenta at E11 (Gekas et al., 2005; Ottersbach and Dzierzak, 2005). Subsequently, at around E11.5, HSPCs migrate to the liver, which is the main site of their expansion and differentiation during fetal life (Mikkola and Orkin, 2006). Finally, from E15.5, these cells colonize the bone marrow, which serves as the main hematopoietic organ in adult life (Cheshier et al., 1999). In the past few decades, a great deal has been learned about the initiation and the differentiation of HSPCs. However, the mechanisms governing the establishment and maintenance of the HSPC pool during ontogeny are less well defined.

Owing to certain embryological and genetic properties, zebrafish have unique advantages for studying vertebrate hematopoiesis. Similar to mice, zebrafish have primitive and definitive waves during the development of hematopoiesis (Davidson and Zon, 2004). In zebrafish, HSPCs arise in the ventral wall of the dorsal aorta (VDA), the zebrafish equivalent of the AGM (Bertrand et al., 2010; Kissa and Herbomel, 2010). Subsequently, these cells migrate to the caudal hematopoietic tissue (CHT) during the fetal stage, and finally colonize the kidney where adult hematopoiesis occurs (Jin et al., 2007; Murayama et al., 2006). Thus, the VDA, CHT and kidney of the zebrafish are respectively the functional analogs of the AGM, liver and bone marrow in mice (Chen and Zon, 2009). Using forward genetic analyses, three previously uncharacterized factors [*rumba* (*znf574*), *haus3* and *cpsfl*] have recently been found to play an essential role in regulating fetal hematopoiesis in zebrafish (Bolli et al., 2011; Du et al., 2011), confirming that the employment of an unbiased forward genetic approach in zebrafish can complement our current knowledge of mammals.

Sumoylation is a post-translational modification that participates in various cellular processes, such as regulation of gene transcription, the cell cycle, genomic integrity, stress responses and organogenesis (Hay, 2005). It involves covalent binding of the small ubiquitin-related modifier (SUMO) to the lysine residues of target proteins via the action of three enzymes (E1, E2 and E3) (Geiss-Friedlander and Melchior, 2007; Mahajan et al., 1997; Matunis et al., 1996). The E1 activating enzyme, a heterodimer of SAE1 and SAE2, catalyzes the C-terminal adenylation of SUMO, followed by the conjugation of adenylylated SUMO to SAE2 via a thioester bond. Subsequently, adenylylated SUMO is trans-esterified from SAE2 to the E2 conjugating enzyme (also known as UBC9). Finally, with the help of E3 ligase, SUMO is conjugated to specific protein substrates and becomes conjugated SUMO. The biological importance of the SUMO pathway has been revealed by genetic studies in various animals. Knockdown of *ubc-9* in *Caenorhabditis elegans* results in embryonic arrest after gastrulation or causes

¹State Key Laboratory of Molecular Neuroscience, Center of Systems Biology and Human Health, Division of Life Science, The Hong Kong University of Science and Technology, Clear Water Bay, Kowloon, Hong Kong, P. R. China. ²Laboratory of Zebrafish Modeling and Drug Screening for Human Diseases of Guangdong Higher Education Institutes, Department of Cell Biology, Southern Medical University, Guangzhou 510515, P. R. China.

*Authors for correspondence (zzwwqq@smu.edu.cn; zilong@ust.hk)

multiple defects of larval development (Jones et al., 2002). In *Drosophila*, the *semushi* mutation of the *ubc9* gene (*lwr* – FlyBase) causes multiple defects in anterior segmentation owing to misregulation of *bicoid* (Epps and Tanda, 1998). Likewise, morpholino oligonucleotide (MO) knockdown of zygotic *ubc9* (*ube2i* – Zebrafish Information Network) in zebrafish results in defects of the craniofacial cartilages, the brain and the eyes (Nowak and Hammerschmidt, 2006), and *Ubc9*-null mice die prior to E7.5 (Nacerddine et al., 2005). More recently, studies in adult mice with inducible *Ubc9* knockout have shown that sumoylation is essential for the survival of stem cells in the intestinal compartment (Demarque et al., 2011). However, detailed characterization of the influence of sumoylation on the hematopoietic phenotype and the mechanism involved requires further investigation.

Here, we report the isolation and characterization of *tango*^{hks5}, a zebrafish mutant with defects of definitive hematopoiesis. Phenotypic characterization of *tango*^{hks5} mutants revealed severely impaired maintenance of HSPCs in the CHT during fetal hematopoiesis. Positional cloning and rescue assay showed that the hematopoietic defect in *tango*^{hks5} is caused by a mutation of the *sae1* gene, which encodes a key component of the E1-activating enzyme. Biochemical analysis revealed that the *tango*^{hks5} mutation leads to synthesis of truncated Sae1, which is less stable and shows weaker binding to Sae2 (Uba2 – Zebrafish Information Network), resulting in systemic reduction of sumoylation. Finally, chimera generation experiments demonstrated that Sae1 acts cell-autonomously. Our findings indicate that the sumoylation pathway is crucial for establishment of the HSPC pool during ontogeny in zebrafish.

MATERIALS AND METHODS

Zebrafish maintenance and ethylnitrosourea (ENU) mutagenesis

Zebrafish were maintained and propagated as described (Westerfield, 1995). AB, WIK, *Tg(cd41:eGFP)* transgenic line (Lin et al., 2005) and *Tg(fli1:eGFP)* fish line (Lawson and Weinstein, 2002) were used in this study. ENU (Sigma) mutagenesis was performed as described previously (Mullins et al., 1994; Solnica-Krezel et al., 1994).

Whole-mount in situ hybridization (WISH)

RNA probes were synthesized using the DIG-RNA Labeling Kit (Roche). WISH was carried out as described previously (Jin et al., 2007).

Terminal deoxynucleotidyl transferase dUTP nick end labeling (TUNEL) assay

TUNEL assay was carried out using the In Situ Cell Death Detection Kit TMR red (Roche) according to the manufacturer's instructions. For the permeability of the whole-mount embryos, embryos were treated with proteinase K (10 mg/ml, Finnzyme) at room temperature (RT) for 105 minutes and then with acetone:ethanol (1:2) mixture at -20°C for 7 minutes. Images were taken using Zeiss LSM 710 DUO confocal microscope.

Bromodeoxyuridine (BrdU) labeling assay and double immunostaining

In brief, 3 days post-fertilization (dpf) *Tg(CD41:eGFP)tango*^{hks5/hks5} mutant embryos and siblings were incubated with 10 mM BrdU (Sigma) for 2.5 hours and then fixed in 4% paraformaldehyde (PFA). After dehydration and rehydration, the embryos were treated with Proteinase K (10 mg/ml, Finnzyme) for 30 minutes at RT and re-fixed in 4% PFA for 30 minutes. After blocking with PBDT (PBS with 0.1% Triton X-100, 1% bovine serum albumen and 1% DMSO), the embryos were stained with goat anti-GFP (Abcam) primary antibody and Alexa Fluor 488-conjugated anti-goat secondary antibodies (Invitrogen). The embryos were fixed again, permeated with Proteinase K for the second time, and re-fixed in 4% PFA. The embryos were then treated with 2 N HCl for 1 hour at RT and stained with anti-BrdU (Roche) and anti-GFP

(Abcam) antibodies. Finally, Alexa Fluor 555-conjugated anti-mouse and Alexa Fluor 488-conjugated anti-goat antibodies (Invitrogen) were used as secondary antibodies to visualize the signals. Images were taken using Zeiss LSM 710 DUO laser scanning confocal microscope.

Positional cloning

Positional cloning was performed as described (Bahary et al., 2004). After screening 1200 *tango*^{hks5/hks5} mutant embryos, the *tango*^{hks5} mutation was mapped to a 130 kb region on chromosome 15 flanked by two simple sequence length polymorphism (SSLP) markers, zk31M14-204059 and zk31M14-68922. Subsequent analysis with single-nucleotide polymorphisms (SNPs) further defined the mutation to a 55 kb region between zk31M14-204059 and zgc154093 SNPs. Direct sequencing of the coding region of the candidate genes identified the *tango*^{hks5} mutation. The primers used for mapping were: z11320 (5'-ACAGGTAAGCAGGGAAAGCT-3', 5'-GCAGAGTCCTTCTGTTTCTCA-3'); z470 (5'-GAGAGCCGAGGTGTGTATGC-3', 5'-CACTGCCTATTACACCACTGATG-3'); zk31M14-204059 (5'-CAGGAACACTCGCATCAAGA-3', 5'-GCTGCTCTCTGACTCCACT-3'); zk31M14-68922 (5'-TGCATT-TTGCCATATATAGATCATT-3', 5'-AGCCAGGTACCCTGGATTAT-3'). The primers used for sequencing zgc154093 SNP were: 5'-GGAT-TGGGAAATGTCACGAG-3', 5'-GCTCTGTCAACCAGGAGGAG-3'. Mutant genotyping was carried out by restriction fragment length polymorphism analysis using enzyme HpyCH4V (NEB).

Plasmid construction and rescue experiment

The *sae1* coding sequence was amplified using primers (5'-CGGG-ATCCCATCTCTCGTCATCATTG-3', 5'-CCGCTCGAGAGTTGACGTGTGGCAAACAG-3') and the PCR product was inserted into the pCS2+ vector. The mutant Δ *sae1* construct was generated from *sae1* wild-type plasmid by overlapping PCR. After linearization by *Not1*, wild-type *sae1* or mutant Δ *sae1* mRNA was synthesized in vitro using Ambion's mMessage mMachine Transcription Kit. Synthesized RNA (~600 pg) was finally injected into each embryo at the 1-cell stage.

Morpholino oligonucleotide (MO) knockdown

The *ubc9* MO (5'-TCGACTCAGAGCAATGCCAGACATG-3') (Gene Tools) was designed as described (Nowak and Hammerschmidt, 2006). *ubc9* MO (~1 pmol) was injected into each wild-type embryo at the 1-cell stage.

Fish protein extraction and western blotting analysis

tango^{hks5/hks5} mutants or wild-type siblings (6 dpf), 20 for each pool, were homogenized in 40 μ l SDS sample buffer (63 mM Tris-HCl, pH 6.8, 10% glycerol, 5% β -mercaptoethanol, 3.5% sodium dodecyl sulfate) and boiled for 5 minutes. After centrifugation at 13,000 rpm (15,700 g) for 10 minutes, supernatant (10 μ l) was loaded for immunoblotting as described previously (Qian et al., 2007). Anti-SUMO-1 (C-terminal) antibody (Sigma, S5446) and anti-SUMO2/3 antibody (Sigma, SAB3500488) were used as the primary antibodies and peroxidase-conjugated donkey anti-rabbit IgG (GE, NA934) was used as the secondary antibody.

Protein expression analysis in 293T cell line

293T cells were cultured in DMEM medium (Gibco) with 10% fetal bovine serum and penicillin-streptomycin (1:100; Invitrogen). Flag-tagged wild-type or mutant Δ *sae1* plasmid (0.1 μ g) was transfected into 293T cells grown in a 6-well plate using Lipofectamine (Invitrogen) according to the manufacturer's instructions. At 24 hours post-transfection, cells were collected and lysed in lysis buffer (150 mM NaCl, 10% glycerol, 50 mM HEPES, pH 7.6, 1.5 mM MgCl₂, 0.1 M NaF, 1 mM EGTA, 1% Triton X-100, protease inhibitor cocktail). For each sample, 5 μ g of total protein lysate was loaded. Anti-Flag (Sigma, F7425) antibody was used to detect the Flag-tagged Sae1.

Quantitative RT-PCR of *sae1* transcript was carried out with total RNA extracted from transfected 293T cells using the RNeasy Mini Kit (Qiagen). Reverse transcription was performed according to the SuperScript III First-Strand Synthesis System (Invitrogen). The primers used for real time PCR were: 5'-CTGTGGATGCAGATGGTTCAG-3', 5'-TCCACTGGTTCA-GTGTCTGC-3'.

Co-immunoprecipitation assay

The coding sequence of zebrafish *sae2* was cloned into pCS2+ vector containing a 6×Myc-tag using primers (5'-GGAATTCAGCAGAACTAGTCGGTCCCTCT-3', 5'-ACGCGTCGACCTAGTCTAGAGCGATGATGT-3'). pCS2+-Myc-*sae2* (0.1 μg) together with 0.1 μg of either wild-type or mutant pCS2+-Flag-*sae1* was co-transfected into 293T cells grown in a 6-well plate. At 24 hours post-transfection, cells were lysed with lysis buffer and centrifuged at 13,000 rpm (15,700 g) for 5 minutes. The supernatants were collected and pre-cleared with 50 μl Protein A/G PLUS-Agarose (Santa Cruz) at 4°C for 1 hour. After removing the beads, the supernatants were mixed with 5 μg anti-Myc antibody (Santa Cruz, 9E10) at 4°C for 1 hour, followed by incubation with 50 μl Protein A/G PLUS-Agarose beads at 4°C for 2 hours. After extensive washing (four times, 15 minutes each), the beads were boiled with 25 μl of 2×Laemmli's buffer and 10 μl of the boiled supernatants were used for western blotting. Flag-Sae1 and Myc-Sae2 were detected using rabbit anti-Flag antibody (Sigma, F7425) and mouse anti-Myc antibody (Santa Cruz, 9E10), respectively.

Chimera generation experiment

Tetramethylrhodamine-labeled dextran (5%; Invitrogen, 10,000 MW) was injected into the donor embryos carrying the *CD41:eGFP* transgene at the one-cell stage. After incubation at 28.5°C for 3 hours, ~30 donor cells were transplanted into the non-transgenic recipient at the 1000-cell stage. The recipients were fixed at 5 dpf, and finally stained with anti-GFP and anti-Hbae1 (α1-globin) antibodies (Du et al., 2011). Images were taken using a Zeiss LSM 510 META laser scanning confocal microscope.

Statistical analysis

Data were analyzed statistically using the two-tailed Student's *t*-test. Results were considered to be significant if $P < 0.05$. Values represent mean ± s.e.m.

RESULTS

tango^{hkz5} mutants show defects of definitive hematopoiesis

As part of our investigations into the genetic network that controls definitive hematopoiesis in vertebrates, we carried out ENU-based forward genetic screening in zebrafish to identify mutants with defects of definitive hematopoiesis. By assessing the thymic expression of recombination-activating gene 1 (*rag1*) (Willett et al., 1997), a dozen *rag1*-deficient mutants were isolated, and *tango*^{hkz5} (Fig. 1A,B) was one of these mutants selected for further investigation. Homozygous *tango*^{hkz5} (*tango*^{hkz5/hkz5}) embryos were morphologically indistinguishable from their siblings at an early stage (data not shown). They had an intact vascular system and normal circulation of blood (data not shown). This was further confirmed by the normal expression of *hbae1* (an erythroid lineage marker) (Brownlie et al., 2003), *lyz* (a myeloid lineage marker) (Liu and Wen, 2002) and *flk1* (an endothelial cell marker; *kdrl* – Zebrafish Information Network) (Fouquet et al., 1997) in *tango*^{hkz5/hkz5} embryos at 25 hours post-fertilization (hpf) (Fig. 1C-H). However, from 5 dpf onwards, *tango*^{hkz5/hkz5} embryos became slimmer and less active than normal embryos, and eventually died at ~10 dpf (data not shown), presumably owing to overwhelming developmental defects.

The lack of T lymphocytes (shown by the absence of *rag1* expression in the thymus), a lineage of definitive origin, prompted us to investigate whether other blood cell lineages related to definitive hematopoiesis were also affected in *tango*^{hkz5} mutants. Whole-mount in situ hybridization (WISH) analysis was employed to examine the expression of *hbae1* and *lyz* at 5 dpf and 6 dpf, which is when definitive erythroid and myeloid cells emerge in the CHT and the kidney (Brownlie et al., 2003; Liu and Wen, 2002). As shown in Fig. 1, strong expression of *hbae1* and *lyz* was

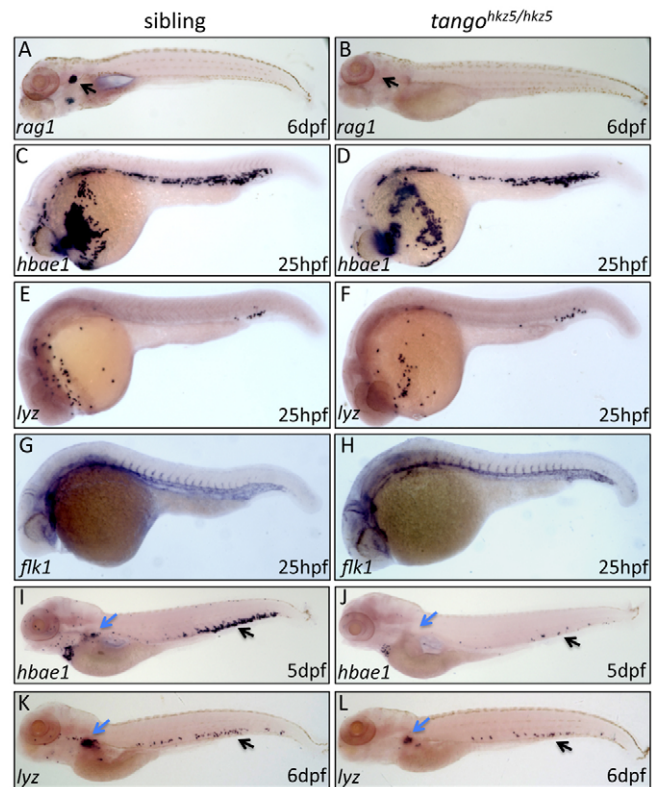


Fig. 1. Impairment of definitive hematopoiesis in *tango*^{hkz5} mutant zebrafish. (A,B) WISH of *rag1* in 6 dpf *tango*^{hkz5/hkz5} embryos and wild-type siblings. Arrows indicate the thymus. (C-H) WISH of *hbae1*, *lyz* and *flk1* in 25 hpf *tango*^{hkz5/hkz5} mutant embryos and wild-type siblings. (I-L) WISH of *hbae1* and *lyz* in 5 dpf and 6 dpf *tango*^{hkz5/hkz5} mutant embryos and wild-type siblings. Blue arrows indicate the position of the kidney; black arrows indicate the CHT.

detected in the CHT and kidney of the control sibling embryos (Fig. 1I,K). By contrast, expression of both markers was considerably reduced in *tango*^{hkz5/hkz5} embryos (Fig. 1J,L). Thus, in addition to the lymphoid lineage, the definitive erythroid and myeloid lineages are also impaired in *tango*^{hkz5} mutants.

The hematopoietic defect in *tango*^{hkz5} mutants is caused by the depletion of HSPCs in the CHT

The impairment of all three major definitive hematopoietic lineages suggested that *tango*^{hkz5} mutants might have a block in the early phase of definitive hematopoiesis, perhaps affecting the development of HSPCs. Previous studies have shown that the development of HSPCs in zebrafish can be followed by the expression of the HSPC-related gene *cmyb* (Jin et al., 2007; Murayama et al., 2006). We therefore examined the generation of HSPCs in the AGM and their subsequent colonization of the CHT, thymus and kidney by monitoring *cmyb* expression in *tango*^{hkz5/hkz5} embryos at various stages of development. We found that the generation of HSPCs in the AGM and their subsequent migration to the CHT were unaffected by the *tango*^{hkz5} mutation, as indicated by normal *cmyb* expression in the AGM of *tango*^{hkz5/hkz5} embryos at 36 hpf (Fig. 2A,B) and in the CHT at 55 hpf (Fig. 2C,D). However, *cmyb* expression in the CHT of *tango*^{hkz5/hkz5} embryos was markedly reduced from 3 dpf onwards (Fig. 2E,F) and was barely detectable by 5 dpf (Fig. 2G-J). Likewise, *cmyb* expression could not be detected in the thymus and kidney (Fig. 2G-J). Similar

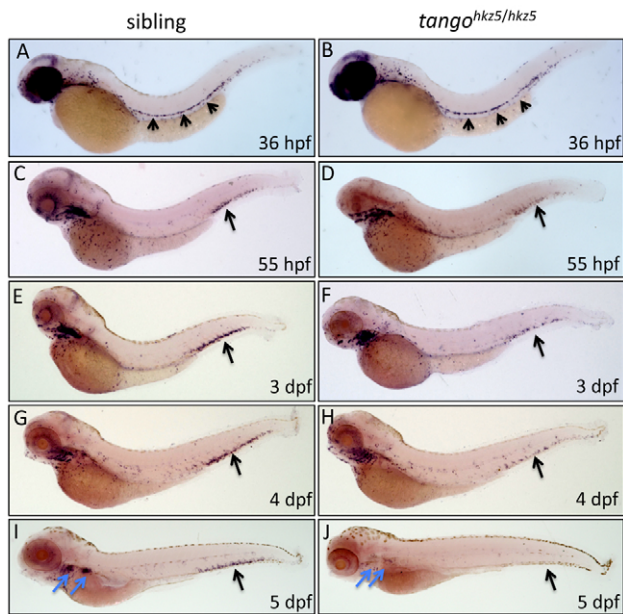


Fig. 2. HSPCs are depleted in the CHT of *tango*^{hkz5} mutant zebrafish. (A–J) WISH of *cmyb* in homozygous mutants of *tango*^{hkz5} and wild-type siblings at 36 hpf (A,B), 55 hpf (C,D) and 3–5 dpf (E,J). Arrows in A and B indicate the AGM region. Black arrows in C–J represent the CHT. The anterior and posterior blue arrows in I–J indicate the thymus and kidney, respectively.

results were obtained in *Tg(CD41:eGFP)tango*^{hkz5/hkz5} transgenic mutant zebrafish. As shown in supplementary material Fig. S1, *CD41-eGFP* positive (*CD41-eGFP*⁺) cells in the CHT, which presumably represent the majority of HSPCs migrated from the AGM (Bertrand et al., 2008; Kissa et al., 2008; Lin et al., 2005), showed ~50% reduction in 3 dpf *Tg(CD41:eGFP)tango*^{hkz5/hkz5} mutant embryos compared with siblings (144 cells vs 249 cells per

embryo) ($P=3.76E-10$, $n=25$) (supplementary material Fig. S1A,B,E), and by 5 dpf *CD41-eGFP*⁺ cells were rarely seen in the CHT of the mutant embryos (supplementary material Fig. S1C,D).

Two possible mechanisms could account for loss of HSPCs from the CHT of *tango*^{hkz5} mutants: enhanced cell death or reduced cell proliferation/cell cycle arrest. To distinguish between these two possibilities, the TUNEL assay was employed to examine the death of HSPCs at 3 dpf when reduction of *CD41-eGFP*⁺ cells in the CHT of *Tg(CD41:eGFP)tango*^{hkz5/hkz5} mutant embryos became apparent (supplementary material Fig. S1). Double staining revealed that the percentage of TUNEL⁺/*CD41-eGFP*⁺ cells in the CHT was significantly increased from 0.2% in siblings to 1.2% in *Tg(CD41:eGFP)tango*^{hkz5/hkz5} mutant embryos (Fig. 3A–E,M; $P=0.002$, $n=13$), indicating that apoptosis of HSPCs was accelerated in *tango*^{hkz5} mutants. However, such a low level (only 1.2% of HSPCs) of cell death suggests that apoptosis is insufficient to account for the drastic reduction of HSPCs in the mutant embryos. We therefore speculated that a proliferation/cell cycle defect might also contribute to the loss of HSPCs in *tango*^{hkz5} mutants. To test this possibility, 3 dpf siblings and *Tg(CD41:eGFP)tango*^{hkz5/hkz5} mutant embryos were incubated with BrdU for 2.5 hours, and the proliferation of HSPCs in the CHT was assessed by double staining with anti-eGFP and anti-BrdU antibodies. The result showed that ~37% of *CD41-eGFP*⁺ cells in sibling embryos were BrdU⁺, whereas the percentage of BrdU⁺ *CD41-eGFP*⁺ cells declined to ~27% in *tango*^{hkz5/hkz5} embryos (Fig. 3G–N; $P=0.0001$, $n=12$). From these studies, we conclude that the failure of developing fetal hematopoiesis in *tango*^{hkz5} mutants is attributed, at least in part, to a combination of increased apoptosis and reduced proliferation of HSPCs. However, other possibilities, such as loss of pluripotency of *CD41-eGFP*⁺ cells, are not excluded.

***tango* encodes the SUMO1-activating enzyme subunit 1**

To identify the genetic change in *tango*^{hkz5} embryos, positional cloning was performed. Bulk segregation analysis revealed that the

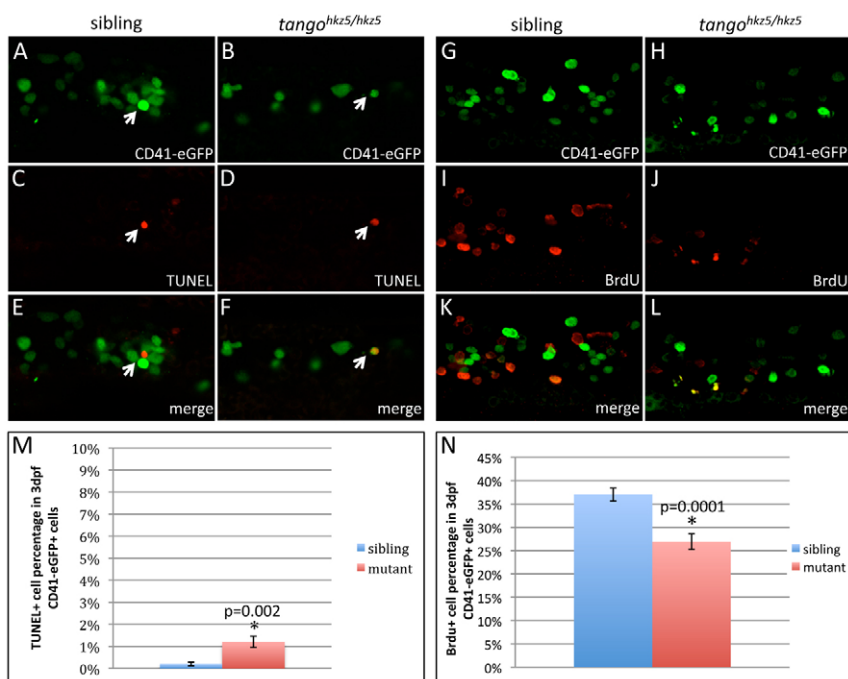


Fig. 3. *tango*^{hkz5} mutation causes an increased apoptosis and a decreased proliferation of HSPCs. (A–F) Double immunostaining of *CD41-eGFP* and TUNEL reveals a slight increase of apoptosis of *CD41-eGFP*⁺ cells in the CHT of 3 dpf *tango*^{hkz5/hkz5} mutant zebrafish embryos. Arrows show the *CD41-eGFP*⁺ and TUNEL⁺ cells. **(G–L)** Double immunostaining of *CD41-eGFP* and BrdU shows a reduced proliferation of *CD41-eGFP*⁺ cells in the CHT of 3 dpf *tango*^{hkz5/hkz5} mutant embryos. **(M)** Quantification of the percentage of TUNEL⁺ cells in the 3 dpf *CD41-eGFP*⁺ cell populations. **(N)** Quantification of the percentage of BrdU⁺ cells in the 3 dpf *CD41-eGFP*⁺ population. Error bars represent s.e.m.

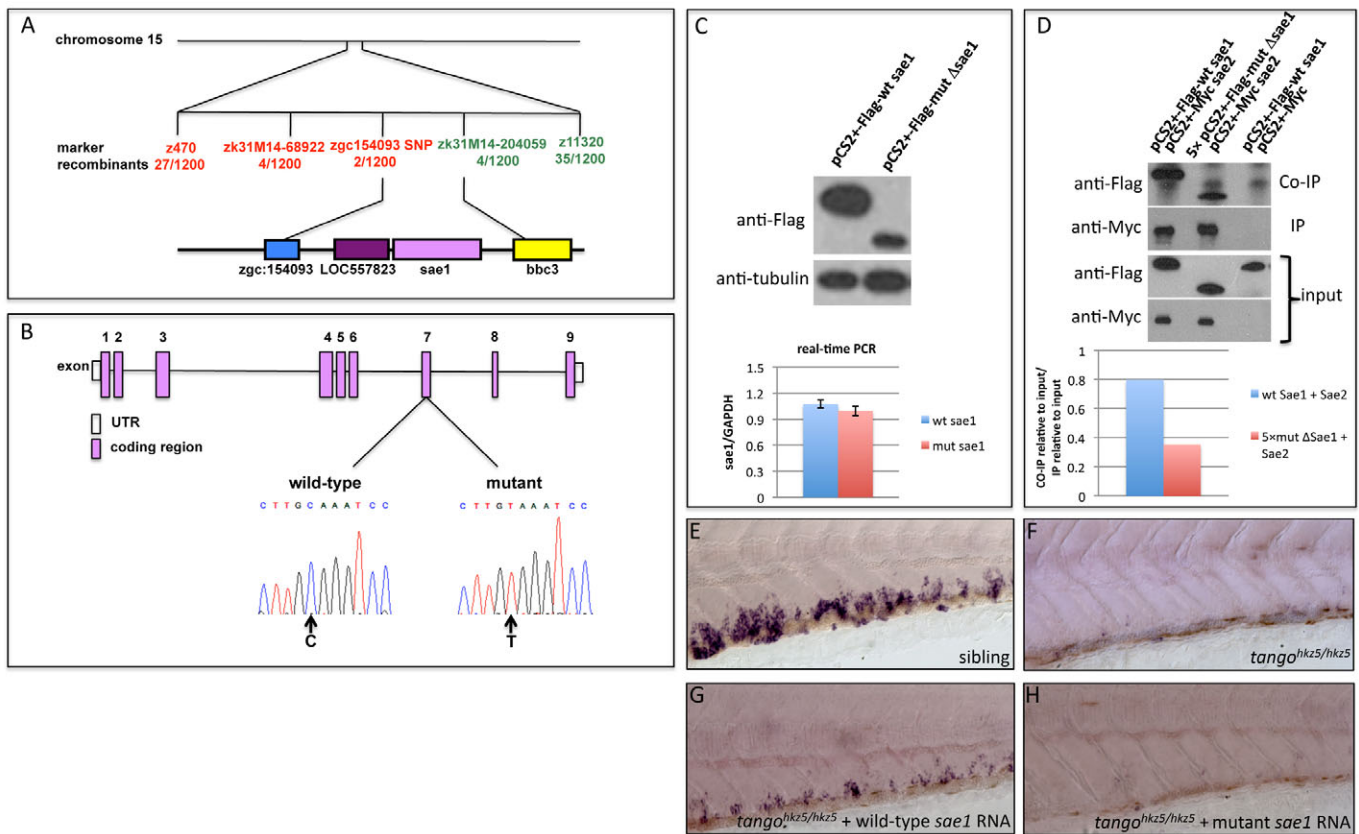


Fig. 4. The *tango*^{hkHz5} mutant phenotype is caused by a nonsense mutation in *sae1*. (A) The *tango*^{hkHz5} mutation was mapped on chromosome 15 between the SNP marker *zgc154093* (two recombinants out of 1200 *tango*^{hkHz5/hkHz5} embryos) and *zk31M14-204059* (four recombinants out of 1200 *tango*^{hkHz5/hkHz5} embryos). This region contains four genes: *sae1*, *LOC557823*, *bbc3* and *zgc154093*. (B) The *sae1* gene contains nine exons and a C-to-T substitution was found in exon 7. (C) Western blotting of 293T cells transfected with pCS2+*Flag-wt sae1* or pCS2+*Flag-mut Δsae1*. The expression level of the mutant ΔSae1 protein was much lower than that of wild-type Sae1. Tubulin was used as a loading control. Real-time PCR showed the similar RNA levels of wild-type and mutant forms of *sae1* relative to *Gapdh* ($P=0.3$, $n=3$). (D) Co-immunoprecipitation assay. 293T cells were co-transfected with either pCS2+*Flag-wt sae1*/pCS2+*Myc-sae2*, or fivefold pCS2+*Flag-mut Δsae1*/pCS2+*Myc-sae2*. Transfection with pCS2+*Flag-wt sae1*/pCS2+*Myc* was used as a negative control. The input showed the similar expression levels of either Flag-Sae1 or Myc-Sae2 between wild type and mutant. Quantification showed that the co-immunoprecipitated mutant ΔSae1 was decreased by >50% compared with wild-type Sae1. The data were reproducible in two independent experiments. (E-H) WISH shows the *cmyb* expression in the CHT of wild-type siblings (E), *tango*^{hkHz5/hkHz5} embryos (F), *tango*^{hkHz5/hkHz5} embryos injected with *sae1* wild-type mRNA (G), and *tango*^{hkHz5/hkHz5} embryos injected with the mutant Δ*sae1* mRNA (H). Error bars represent s.e.m.

tango^{hkHz5} mutation was located on chromosome 15 and fine-mapping analysis further localized the mutation to a 55 kb region containing four genes: SUMO1-activating enzyme subunit 1 (*sae1*), *LOC557823*, *bbc3* and *zgc154093* (Fig. 4A). Sequencing of the coding regions of these four genes identified a single nonsense mutation in exon 7 of the *sae1* gene (Fig. 4B), which encodes a key subunit of the E1 enzyme required for sumoylation. Protein sequence alignment revealed that Sae1 is highly conserved among humans, mice, rats and zebrafish (supplementary material Fig. S2). The mutation creates a stop codon at amino acid Q273 (Q273X), resulting in the synthesis of a truncated Sae1 protein (ΔSae1) lacking the C-terminal 76 amino acids. Biochemical analysis showed that this truncated ΔSae1 protein was unstable because its expression level was significantly lower than that of the wild-type protein, despite their similar RNA levels shown by real-time PCR after transfection into 293T cells (Fig. 4C). Moreover, co-immunoprecipitation assay showed that the binding of truncated ΔSae1 with Sae2 was also reduced (Fig. 4D). These data suggest that the Q273X mutation of *sae1* disrupts the sumoylation pathway

by both reducing the stability of Sae1 protein and affecting its interaction with Sae2.

To confirm that the hematopoiesis defect in *tango*^{hkHz5} mutants was indeed caused by the loss of Sae1 function, we carried out rescue experiments with in vitro synthesized wild-type *sae1* mRNA or mutant Δ*sae1* mRNA. Injection of wild-type *sae1* mRNA into the *tango*^{hkHz5/hkHz5} mutant embryos partially restored fetal hematopoiesis as shown by the reappearance of *cmyb* expression in the CHT (Fig. 4E-G; 28/45). By contrast, injection of mutant Δ*sae1* RNA (0/25) did not restore *cmyb* expression (Fig. 4E,F,H). Taken together, these results demonstrate that the Q273X mutation in the *sae1* gene did indeed cause a definitive hematopoietic defect in *tango*^{hkHz5} mutants.

The sumoylation pathway is disrupted by the Sae1 mutation in *tango*^{hkHz5} mutants

As Sae1 is a key component of the sumoylation pathway, we hypothesized that the hematopoietic phenotype of *tango*^{hkHz5} mutants was probably related to impaired protein sumoylation. To support

this hypothesis, we first knocked down the expression of zygotic *ubc9* with morpholino oligonucleotides (MOs) (Corey and Abrams, 2001) to determine whether suppression of another key factor in the sumoylation pathway would cause a similar hematopoietic phenotype to that of *tango^{hkz5}*. As expected, primitive hematopoiesis was not affected by *Ubc9* knockdown (Fig. 5A-D). Neither was the initiation of HSPCs in the VDA and their subsequent mobilization to the CHT (Fig. 5A-F). However, HSPCs were not sustained in the CHT, as indicated by reduced *cmyb* expression in 3 dpf and 4 dpf *ubc9* MO knockdown embryos (morphants) (Fig. 5G-J). The similar hematopoietic defects in *tango^{hkz5}* mutants and *ubc9* morphants suggest that the *tango^{hkz5}* phenotype is probably caused by suppression of sumoylation.

To support the notion that the sumoylation pathway was defective in *tango^{hkz5}* mutants, we extracted total protein from 6 dpf *tango^{hkz5/hkz5}* embryos and determined the levels of free and conjugated SUMOs. There are three SUMO paralogs in zebrafish, SUMO1, SUMO2 and SUMO3, which exist as both free and conjugated forms. We reasoned that the defect of sumoylation in *tango^{hkz5}* mutants would lead to a decrease of conjugated SUMOs and an increase of free SUMOs. Western blotting with anti-SUMO1 and anti-SUMO2/3 antibodies showed that the level of free SUMO1 and SUMO2/3 was increased in *tango^{hkz5/hkz5}* embryos. As anticipated, SUMO2/3 conjugates were found to be reduced in *tango^{hkz5/hkz5}* embryos compared with their siblings, although the change of SUMO1 conjugates was minimal (Fig. 5K-

N). This result is similar to that observed in inducible *Ubc9* knockout mice (Demarque et al., 2011). From these observations, we conclude that sumoylation pathway is indeed severely impaired in *tango^{hkz5}* mutants.

Sae1 is cell-autonomously required for the maintenance of HSPCs in the CHT

To explore how *sae1* affects the maintenance of HSPCs in the CHT, we first examined the temporal and spatial expression pattern of *sae1* during zebrafish embryogenesis. WISH analysis revealed that *sae1* was widely distributed in the embryonic body, and was particularly prominent in the brain (supplementary material Fig. S3). The ubiquitous expression of *sae1* raised the question of whether the hematopoietic defects in *tango^{hkz5}* mutants were caused by a cell-autonomous or non-cell-autonomous effect. To clarify these two possibilities, chimera generation experiments were performed with *Tg(CD41:eGFP)* transgenic zebrafish, in which HSPCs are preferentially labeled by eGFP (Lin et al., 2005). We first injected wild-type cells from 3 hpf *Tg(CD41:eGFP)* transgenic embryos into either 3 hpf *tango^{hkz5/hkz5}* embryos or 3 hpf sibling embryos, and the contribution of donor cells to HSPCs was scored at 5 dpf by calculating the number of GFP-positive cells in the CHT. The result showed that ~13.7% (10/73) of the 5 dpf *tango^{hkz5/hkz5}* hosts contained *CD41-eGFP⁺* wild-type donor cells in the CHT, a proportion comparable to that in sibling hosts (15.1%; 36/238 embryos) (Fig. 6A,B; Table 1). The contribution of

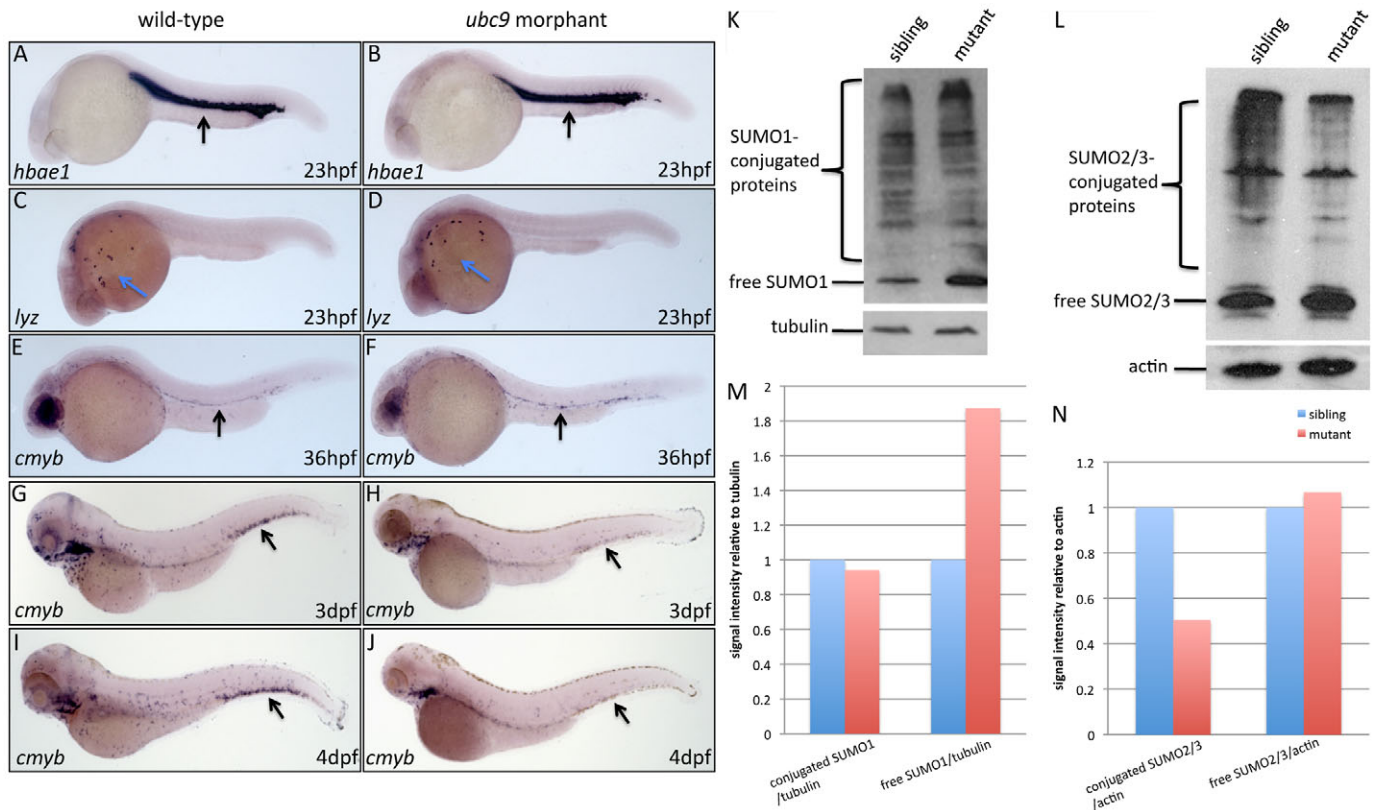


Fig. 5. Loss of Sae1 function impairs the sumoylation pathway. (A-D) WISH shows the *hbae1* and *lyz* expression in 23 hpf wild-type fish and *ubc9* morphants. Black arrows indicate the ICM. Blue arrows indicate the yolk sac. (E,F) WISH indicates the *cmyb* expression in 36 hpf wild-type fish and *ubc9* morphants. Arrows indicate the CHT region. (G-J) WISH shows the *cmyb* expression in 3-4 dpf wild-type fish and *ubc9* morphants. Arrows indicate the CHT region. (K) Western blotting indicates the expression of free SUMO1s and the SUMO1 conjugates in 6 dpf siblings (left) and *tango^{hkz5/hkz5}* mutant embryos (right). (L) Western blotting shows the expression of free SUMO2/3 and the SUMO2/3 conjugates in 6 dpf siblings (left) and *tango^{hkz5/hkz5}* mutant embryos (right). (M) Quantification of the SUMO1 conjugates and the free SUMO1 relative to tubulin. (N) Quantification of the SUMO2/3 conjugates and the free SUMO2/3 relative to actin.

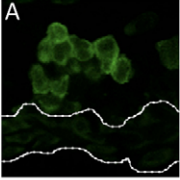
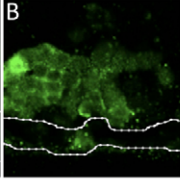
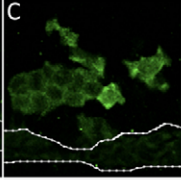
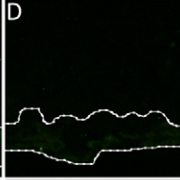
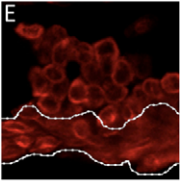
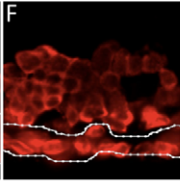
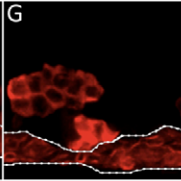
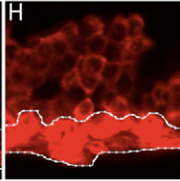
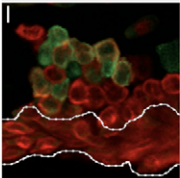
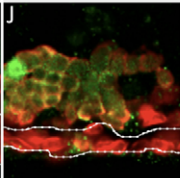
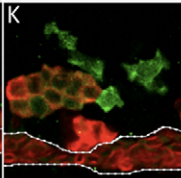
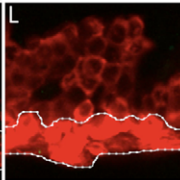
Donor	wild-type	wild-type	sibling	<i>tango</i> ^{hkz5/hkz5}
Host	sibling	<i>tango</i> ^{hkz5/hkz5}	wild-type	wild-type
ratio	15.1% (36/238)	13.7% (10/73)	9.6% (20/209)	0% (0/59)
CD41-eGFP				
Hbae1				
merge				

Fig. 6. Sae1 cell-autonomously regulates HSPC survival in the CHT. (A-D) Immunofluorescence staining of GFP in the CHT of 5 dpf host fish. (E-H) Immunofluorescence staining of Hbae1 in the CHT of 5 dpf host fish. (I-L) Merged images of GFP and Hbae1 immunofluorescence staining. A, E and I are the *tango*^{hkz5} sibling hosts transplanted with wild-type cells carrying *CD41-eGFP*. B, F and J are the *tango*^{hkz5/hkz5} mutants transplanted with wild-type cells carrying *CD41-eGFP*. C, G and K are the wild-type fish transplanted with *tango*^{hkz5} sibling cells carrying *CD41-eGFP*. D, H and L are the wild-type fish transplanted with *tango*^{hkz5/hkz5} mutant cells carrying *CD41-eGFP*. White dotted lines indicate the caudal vein.

wild-type donor cells to the *CD41-eGFP*⁺ cells in the chimera hosts was also comparable between sibling (0.2-15.4%) and *tango*^{hkz5/hkz5} hosts (0.8-36.8%) (Table 1). The slightly higher percentage for wild type into mutant hosts is possibly due to a compensation effect, in which the functional niche in the mutants might impose a positive feedback loop when healthy donors successfully dock into their niche. Moreover, the implanted donor *CD41-eGFP*⁺ cells were capable of differentiating into erythrocytes, as shown by co-immunostaining with Hbae1 (Fig. 6E,F,I,J), demonstrating that the microenvironment in the mutant CHT is capable of supporting the growth and differentiation of wild-type hematopoietic cells. Consistent with this notion, anti-GFP staining of *Tg(fli1:eGFP)tango*^{hkz5} mutants, in which the vascular structure is labeled by GFP expression (Lawson and Weinstein, 2002), revealed intact vascular plexuses in the CHT (supplementary material Fig. S4). Collectively, these results strongly suggest that the defect of hematopoiesis in *tango*^{hkz5} mutants is probably caused by a cell-autonomous effect. To confirm this, cells derived from *Tg(cd41:eGFP)tango*^{hkz5/hkz5} embryos or their siblings were transplanted into wild-type hosts. The result showed that ~9.6% (20/209) of the wild-type recipients showed engraftment of *CD41-eGFP*⁺ sibling cells capable of differentiating into the erythroid lineage (Fig. 6C,G,K; Table 1). However, none of the 59 wild-type recipients showed engraftment of mutant donor cells (Fig. 6D,H,L; Table 1), despite the fact that

the mutant donor cells were capable of contributing to non-hematopoietic tissue, such as muscle (53.8% vs 53.5% for the percentage of recipients containing donor cells; 0.4-6.3% vs 0.2-5.9% for percentage chimerism) and CNS (56.4% vs 55.9% for the percentage of recipients containing donor cells), as potentially as did the sibling donor cells (supplementary material Table S1). Taken together, these bi-directional transplantation assays demonstrate that Sae1 is cell-autonomously required for the maintenance of HSPCs in the CHT.

DISCUSSION

In this study, we identified a zebrafish mutant with defects of definitive hematopoiesis that were particularly related to maintenance of HSPCs in the CHT. This phenotype was caused by a nonsense mutation of the *sae1* gene, a subunit of E1 enzyme involved in the sumoylation of proteins. Further investigation revealed that the *sae1* gene product was cell-autonomously required for the development of HSPCs during fetal hematopoiesis.

Consistent with the conservation of the sumoylation pathway, SAE1 protein shows a high degree of similarity among various species, including humans, mice, rats and zebrafish. The structure of human SAE1 has been determined and it consists of ten β -sheets and eleven α -helices (Lois and Lima, 2005). Several regions and amino acids essential for SAE1 activity have been identified

Table 1. Summary of chimera generation experiments (contribution to hematopoietic cells)

Donor (<i>CD41-eGFP</i> ⁺ transgenic fish)	Host (AB fish)	Total number of host embryos	Number of host embryos with donor-derived <i>CD41-eGFP</i> ⁺ cells	Subgroup of host embryos with donor-derived <i>CD41-eGFP</i> ⁺ cells			Percentage of donor-derived <i>CD41-eGFP</i> ⁺ cells in the host CHT*
				1-20 <i>CD41-eGFP</i> ⁺ cells	21-50 <i>CD41-eGFP</i> ⁺ cells	>50 <i>CD41-eGFP</i> ⁺ cells	
Wild type	Sibling	238	36 (15.1%)	13	15	8	0.2-15.4%
Wild type	<i>tango</i> ^{hkz5/hkz5}	73	10 (13.7%)	2	5	3	0.8-36.8%
Sibling	Wild type	209	20 (9.6%)	11	7	2	0.8-16.2%
<i>tango</i> ^{hkz5/hkz5}	Wild type	59	0	0	0	0	0%

*The number of *CD41-eGFP*⁺ cells in 5 dpf wild-type CHT is ~500.

through the study of various SAE1 mutants (Schulman and Harper, 2009). The N-terminal amino acids 1-27 and the RLW motif (Arg21, Arg24, Leu25 and Trp26 side chains) of SAE1 are required for SAE1/SAE2 adenylation (Olsen et al., 2010). However, the domain mediating the physical interaction between SAE1 and SAE2 to form the functional E1 enzyme has not been defined. Our study showing that the truncated Δ Sae1 protein lacking the C-terminal 76 amino acids showed a decrease of binding to Sae2, indicating that the C-terminal region, which forms two β -sheets and two α -helices (Lois and Lima, 2005), is involved in assembly of the Sae1/Sae2 heterodimer.

WISH analysis revealed that *sae1* expression is not restricted to hematopoietic tissues and is ubiquitously expressed in many tissues, showing that Sae1 acts as a systemic sumoylation factor. However, *tango*^{h_{kz}5/h_{kz}5} mutant embryos showed no obvious morphological abnormalities during early development. The lack of more widespread developmental defects during early embryogenesis of *tango*^{h_{kz}5/h_{kz}5} embryos may have been due to the influence of maternal *sae1* mRNA. In fact, as the *tango*^{h_{kz}5/h_{kz}5} embryos continued to develop to later stages, various abnormalities began to emerge, including defects of the CNS due to massive cell death in the brain, eyes and spinal cord (data not shown). Notably, both the hematopoietic tissue and CNS show rapid proliferation during early stage of development, suggesting that the sumoylation pathway might be more important for actively proliferating cells.

The hematopoietic defect in *tango*^{h_{kz}5} mutants is caused by suppression of sumoylation pathway, as indicated by the increase of free SUMOs and decrease of conjugated SUMOs in homozygous *tango*^{h_{kz}5/h_{kz}5} embryos. Given that the failure of fetal hematopoiesis in *tango*^{h_{kz}5} mutants is attributable to the combined effect of accelerated apoptosis and diminished proliferation of HSPCs, we speculate that the downstream targets affected by the Sae1 Q273X mutation are likely to be those involved in apoptosis and/or cell cycle regulation. Among various potential targets, p53, an essential regulator of apoptosis and cell proliferation, appears to be a candidate because sumoylation of p53 has been reported to modulate its transcription activity (Gostissa et al., 1999; Rodriguez et al., 1999; Schmidt and Müller, 2002; Wu and Chiang, 2009). Another subclass of molecules potentially affected by the Sae1 Q273X mutation is those involved in DNA replication, including origin recognition complex 3, topoisomerase 1 and DNA replication helicase 2, as their activity is also modulated by sumoylation (Makhnevych et al., 2009). Further investigation will be required to identify the underlying molecular mechanism.

Finally, investigation of sumoylation in *tango*^{h_{kz}5} mutants demonstrates an increase of free SUMOs (SUMO1 and SUMO2/3) and a decrease of SUMO2/3 conjugates, although SUMO1 conjugates were almost unchanged. This observation is consistent with the results from a study of *Ubc9* knockout mice, which revealed an increase of free SUMO1 and a decrease of conjugated SUMO2, but no change of SUMO1-modified substrates, in *Ubc9*-deficient embryonic fibroblasts (Demarque et al., 2011). Collectively, the results obtained in *Ubc9* knockout mice and our current findings in zebrafish suggest that suppression of either Sae1 or E2 activity affects SUMO2 conjugation more profoundly than it affects SUMO1 conjugation.

Acknowledgements

We thank R. Handin for providing *Tg(cd41:eGFP)* transgenic line.

Funding

This work was supported by the National Basic Research Program of China [grant 2012CB945102]; the National Natural Science Foundation of China

[grant 31171403]; and General Research Fund (GRF) grants from the Research Grants Council of the Hong Kong Special Administrative Region (HKSAR) [grants 663109, 663111 and HKUST6/CRF/09].

Author contributions

X.L., Y.L. and J.X. designed the research, performed experiments and analyzed data. W.Z. and Z.W. designed the research and analyzed data.

Competing interests statement

The authors declare no competing financial interests.

Supplementary material

Supplementary material available online at <http://dev.biologists.org/lookup/suppl/doi:10.1242/dev.081869/-/DC1>

References

- Bahary, N., Davidson, A., Ransom, D., Shepard, J., Stern, H., Trede, N., Zhou, Y., Barut, B. and Zon, L. I. (2004). The Zon laboratory guide to positional cloning in zebrafish. *Methods Cell Biol.* **77**, 305-329.
- Bertrand, J. Y., Kim, A. D., Teng, S. and Traver, D. (2008). CD41+ cmyb+ precursors colonize the zebrafish pronephros by a novel migration route to initiate adult hematopoiesis. *Development* **135**, 1853-1862.
- Bertrand, J. Y., Chi, N. C., Santoso, B., Teng, S., Stainier, D. Y. and Traver, D. (2010). Haematopoietic stem cells derive directly from aortic endothelium during development. *Nature* **464**, 108-111.
- Bolli, N., Payne, E. M., Rhodes, J., Gjini, E., Johnston, A. B., Guo, F., Lee, J. S., Stewart, R. A., Kanki, J. P., Chen, A. T. et al. (2011). *cpsf1* is required for definitive HSC survival in zebrafish. *Blood* **117**, 3996-4007.
- Brownlie, A., Hersey, C., Oates, A. C., Paw, B. H., Falick, A. M., Witkowska, H. E., Flint, J., Higgs, D., Jessen, J., Bahary, N. et al. (2003). Characterization of embryonic globin genes of the zebrafish. *Dev. Biol.* **255**, 48-61.
- Chen, A. T. and Zon, L. I. (2009). Zebrafish blood stem cells. *J. Cell. Biochem.* **108**, 35-42.
- Cheshier, S. H., Morrison, S. J., Liao, X. and Weissman, I. L. (1999). In vivo proliferation and cell cycle kinetics of long-term self-renewing hematopoietic stem cells. *Proc. Natl. Acad. Sci. USA* **96**, 3120-3125.
- Corey, D. R. and Abrams, J. M. (2001). Morpholino antisense oligonucleotides: tools for investigating vertebrate development. *Genome Biol.* **2**, Reviews 1015.1-1015.3.
- Cumano, A. and Godin, I. (2007). Ontogeny of the hematopoietic system. *Annu. Rev. Immunol.* **25**, 745-785.
- Davidson, A. J. and Zon, L. I. (2004). The 'definitive' (and 'primitive') guide to zebrafish hematopoiesis. *Oncogene* **23**, 7233-7246.
- Demarque, M. D., Nacerddine, K., Neyret-Kahn, H., Andrieux, A., Danenberg, E., Jouvion, G., Bomme, P., Hamard, G., Romagnolo, B., Terris, B. et al. (2011). Sumoylation by Ubc9 regulates the stem cell compartment and structure and function of the intestinal epithelium in mice. *Gastroenterology* **140**, 286-296.
- Du, L., Xu, J., Li, X., Ma, N., Liu, Y., Peng, J., Osato, M., Zhang, W. and Wen, Z. (2011). Rumba and Haus3 are essential factors for the maintenance of hematopoietic stem/progenitor cells during zebrafish hematopoiesis. *Development* **138**, 619-629.
- Epps, J. L. and Tanda, S. (1998). The *Drosophila* *semushi* mutation blocks nuclear import of bicoid during embryogenesis. *Curr. Biol.* **8**, 1277-1280.
- Fouquet, B., Weinstein, B. M., Serluca, F. C. and Fishman, M. C. (1997). Vessel patterning in the embryo of the zebrafish: guidance by notochord. *Dev. Biol.* **183**, 37-48.
- Galloway, J. L. and Zon, L. I. (2003). Ontogeny of hematopoiesis: examining the emergence of hematopoietic cells in the vertebrate embryo. *Curr. Top. Dev. Biol.* **53**, 139-158.
- Geiss-Friedlander, R. and Melchior, F. (2007). Concepts in sumoylation: a decade on. *Nat. Rev. Mol. Cell Biol.* **8**, 947-956.
- Gekas, C., Dieterlen-Lievre, F., Orkin, S. H. and Mikkola, H. K. A. (2005). The placenta is a niche for hematopoietic stem cells. *Dev. Cell.* **8**, 365-375.
- Gostissa, M., Hengstermann, A., Fogal, V., Sandy, P., Schwarz, S. E., Scheffner, M. and Del Sal, G. (1999). Activation of p53 by conjugation to the ubiquitin-like protein SUMO-1. *EMBO J.* **18**, 6462-6471.
- Haar, J. L. and Ackerman, G. A. (1971). A phase and electron microscopic study of vasculogenesis and erythropoiesis in the yolk sac of the mouse. *Anat. Rec.* **170**, 199-223.
- Hay, R. T. (2005). SUMO: a history of modification. *Mol. Cell* **18**, 1-12.
- Jin, H., Xu, J. and Wen, Z. (2007). Migratory path of definitive hematopoietic stem/progenitor cells during zebrafish development. *Blood* **109**, 5208-5214.
- Jones, D., Crowe, E., Stevens, T. A. and Candido, E. P. (2002). Functional and phylogenetic analysis of the ubiquitylation system in *Caenorhabditis elegans*: ubiquitin-conjugating enzymes, ubiquitin-activating enzymes, and ubiquitin-like proteins. *Genome Biol.* **3**, RESEARCH0002.
- Kissa, K. and Herbomel, P. (2010). Blood stem cells emerge from aortic endothelium by a novel type of cell transition. *Nature* **464**, 112-115.

- Kissa, K., Murayama, E., Zapata, A., Cortés, A., Perret, E., Machu, C. and Herbomel, P. (2008). Live imaging of emerging hematopoietic stem cells and early thymus colonization. *Blood* **111**, 1147-1156.
- Lawson, N. D. and Weinstein, B. M. (2002). In vivo imaging of embryonic vascular development using transgenic zebrafish. *Dev. Biol.* **248**, 307-318.
- Lin, H. F., Traver, D., Zhu, H., Dooley, K., Paw, B. H., Zon, L. I. and Handin, R. I. (2005). Analysis of thrombocyte development in CD41-GFP transgenic zebrafish. *Blood* **106**, 3803-3810.
- Liu, F. and Wen, Z. (2002). Cloning and expression pattern of the lysozyme C gene in zebrafish. *Mech. Dev.* **113**, 69-72.
- Lois, L. M. and Lima, C. D. (2005). Structures of the SUMO E1 provide mechanistic insights into SUMO activation and E2 recruitment to E1. *EMBO J.* **24**, 439-451.
- Mahajan, R., Delphin, C., Guan, T. L., Gerace, L. and Melchior, F. (1997). A small ubiquitin-related polypeptide involved in targeting RanGAP1 to nuclear pore complex protein RanBP2. *Cell* **88**, 97-107.
- Makhnevych, T., Sydorsky, Y., Xin, X., Srikumar, T., Vizeacoumar, F. J., Jeram, S. M., Li, Z., Bahr, S., Andrews, B. J., Boone, C. et al. (2009). Global map of SUMO function revealed by protein-protein interaction and genetic networks. *Mol. Cell* **33**, 124-135.
- Matunis, M. J., Coutavas, E. and Blobel, G. (1996). A novel ubiquitin-like modification modulates the partitioning of the Ran-GTPase-activating protein RanGAP1 between the cytosol and the nuclear pore complex. *J. Cell Biol.* **135**, 1457-1470.
- Medvinsky, A. and Dzierzak, E. (1996). Definitive hematopoiesis is autonomously initiated by the AGM region. *Cell* **86**, 897-906.
- Mikkola, H. K. and Orkin, S. H. (2006). The journey of developing hematopoietic stem cells. *Development* **133**, 3733-3744.
- Mullins, M. C., Hammerschmidt, M., Haffter, P. and Nüsslein-Volhard, C. (1994). Large-scale mutagenesis in the zebrafish: in search of genes controlling development in a vertebrate. *Curr. Biol.* **4**, 189-202.
- Murayama, E., Kissa, K., Zapata, A., Mordelet, E., Briolat, V., Lin, H. F., Handin, R. I. and Herbomel, P. (2006). Tracing hematopoietic precursor migration to successive hematopoietic organs during zebrafish development. *Immunity* **25**, 963-975.
- Nacerddine, K., Lehembre, F., Bhaumik, M., Artus, J., Cohen-Tannoudji, M., Babinet, C., Pandolfi, P. P. and Dejean, A. (2005). The SUMO pathway is essential for nuclear integrity and chromosome segregation in mice. *Dev. Cell.* **9**, 769-779.
- Nowak, M. and Hammerschmidt, M. (2006). Ubc9 regulates mitosis and cell survival during zebrafish development. *Mol. Biol. Cell* **17**, 5324-5336.
- Olsen, S. K., Capili, A. D., Lu, X., Tan, D. S. and Lima, C. D. (2010). Active site remodelling accompanies thioester bond formation in the SUMO E1. *Nature* **463**, 906-912.
- Ottersbach, K. and Dzierzak, E. (2005). The murine placenta contains hematopoietic stem cells within the vascular labyrinth region. *Dev. Cell* **8**, 377-387.
- Qian, F., Zhen, F., Xu, J., Huang, M., Li, W. and Wen, Z. (2007). Distinct functions for different scl isoforms in zebrafish primitive and definitive hematopoiesis. *PLoS Biol.* **5**, e132.
- Rodriguez, M. S., Desterro, J. M., Lain, S., Midgley, C. A., Lane, D. P. and Hay, R. T. (1999). SUMO-1 modification activates the transcriptional response of p53. *EMBO J.* **18**, 6455-6461.
- Schmidt, D. and Müller, S. (2002). Members of the PIAS family act as SUMO ligases for c-Jun and p53 and repress p53 activity. *Proc. Natl. Acad. Sci. USA* **99**, 2872-2877.
- Schulman, B. A. and Harper, J. W. (2009). Ubiquitin-like protein activation by E1 enzymes: the apex for downstream signalling pathways. *Nat. Rev. Mol. Cell Biol.* **10**, 319-331.
- Solnica-Krezel, L., Schier, A. F. and Driever, W. (1994). Efficient recovery of ENU-induced mutations from the zebrafish germline. *Genetics* **136**, 1401-1420.
- Takahashi, K., Yamamura, F. and Naito, M. (1989). Differentiation, maturation, and proliferation of macrophages in the mouse yolk sac: a light-microscopic, enzyme-cytochemical, immunohistochemical, and ultrastructural study. *J. Leukoc. Biol.* **45**, 87-96.
- Westerfield, M. (1995). *The Zebrafish Book: A Guide for the Laboratory Use of Zebrafish (Danio rerio)*, 3rd edn. Eugene, OR: University of Oregon Press.
- Willet, C. E., Cherry, J. J. and Steiner, L. A. (1997). Characterization and expression of the recombination activating genes (rag1 and rag2) of zebrafish. *Immunogenetics* **45**, 394-404.
- Wu, S. Y. and Chiang, C. M. (2009). Crosstalk between sumoylation and acetylation regulates p53-dependent chromatin transcription and DNA binding. *EMBO J.* **28**, 1246-1259.

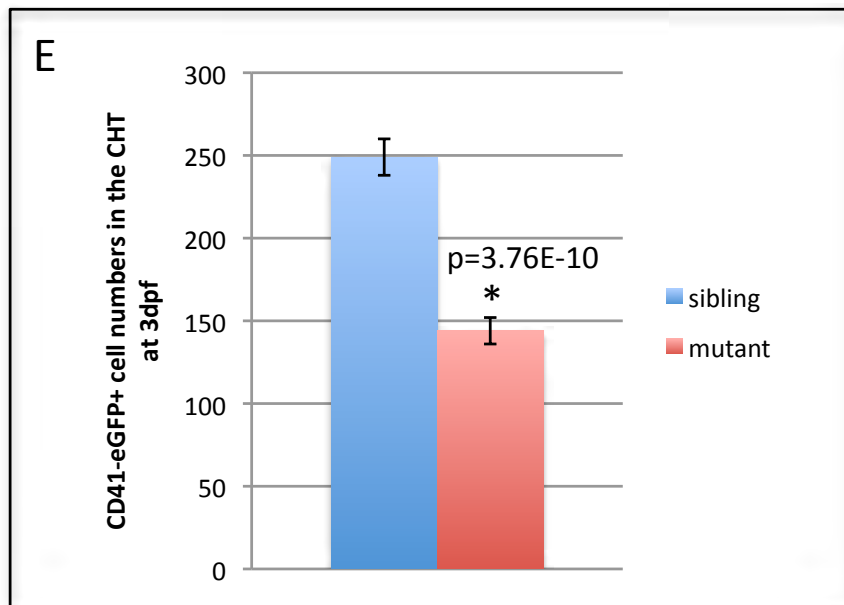
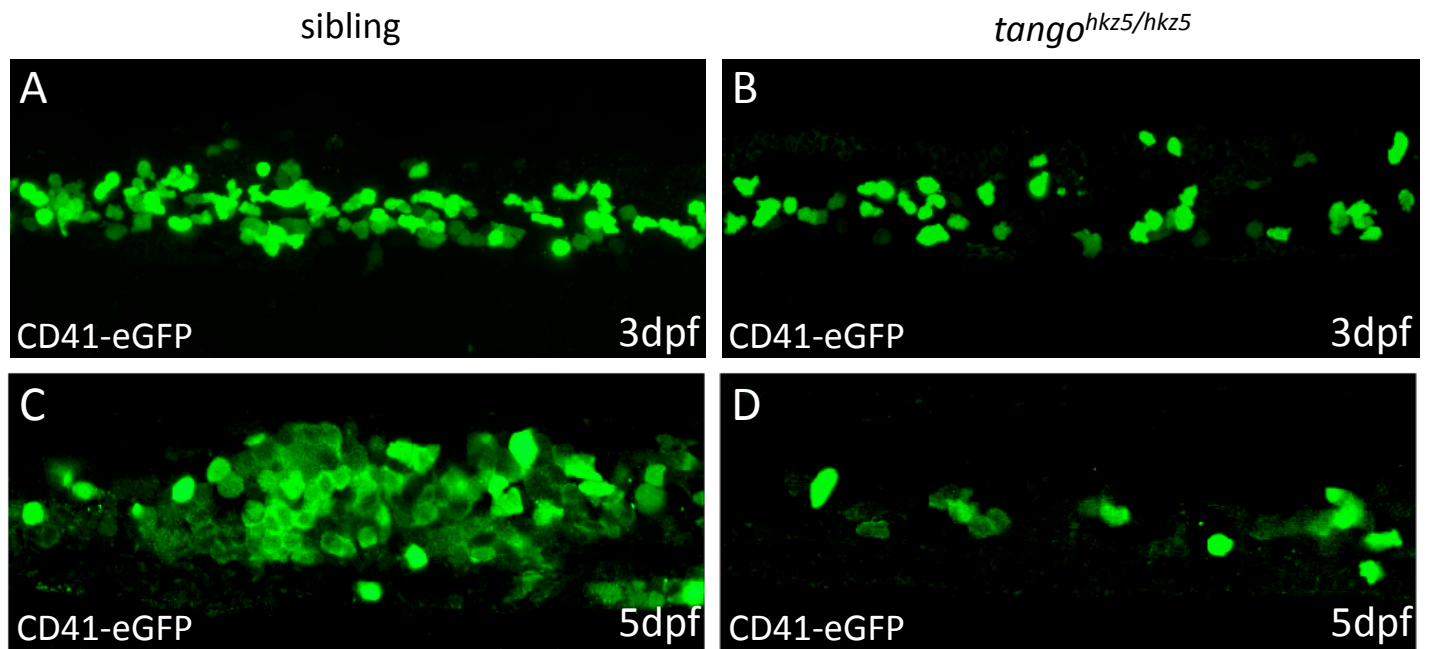


Fig. S1. *CD41-eGFP*⁺ HSPCs are reduced in the CHT of *tango*^{hkz5} mutants. (A-D) Immunostaining of eGFP in the CHT of *tango*^{hkz5/hkz5} mutant embryos and their siblings at 3 dpf and 5 dpf. (E) Quantification of *CD41-eGFP*⁺ cell number in the CHT of 3 dpf *tango*^{hkz5/hkz5} mutant embryos and siblings. Error bars represent s.e.m.

```

*:. * . *****:*****.***:*.***:*****.*****.*****
mouseNP_062722 MVEKEEAGGGGGGISEEEAAQYDROI RLWGLEAQKRLRASRV LIVGMKGLGAEIAKNLILAGVKGLTMLDHEOV 75
ratNP_001012063 MVEKEEVSGGGG-ISEEEAAQYDROI RLWGLEAQKRLRASRV LIVGMKGLGAEIAKNLILAGVKGLTMLDHEOV 74
humanNP_005491.1 MVEKEEAGGG----ISEEEAAQYDROI RLWGLEAQKRLRASRV LLVGLRGLGAEIAKNLILAGVKGLTMLDHEOV 71
zebrafishNP_001002058.1 MIDTIEKEDT---ISEEEAAQYDROI RLWGLDAQKRLRGRSV LLVGLRGLGAEVAKNLILAGVKGLTLLDHEOV 72

: * . ***** ..*:***** *****.***.*** :*:*:* *:*:*:* *:*:*:* *:*:*:*
mouseNP_062722 SPEDPGAQFLIQTGSVGRNRAEASLERAQNLNPMVDVKVDTE DVEKKPESFFTKF DAVCLTCCSRDVIKVDQIC 150
ratNP_001012063 SPEDLGAQFLIRTG SVGNRAEASLERAQNLNPMVDVKVDTE DVEKKPESFFTEF DAVCLTCCSKDVIKVDQIC 149
humanNP_005491.1 TPEDPGAQFLIRTG SVGRNRAEASLERAQNLNPMVDVKVDTE DVEKKPESFFTF DAVCLTCCSRDVIKVDQIC 146
zebrafishNP_001002058.1 TEESRRAQFLIPVDADGONHAQASLERAQFLNPMVEVKADTE PVEKPPDDFFFQ DAVCLTRCSRDLMVRVDQLC 147

..**.* **:*:* **:* *:*:* *:*:* *:*:* *:*:* *:*:* *:*:* *:*:* *:*:* *:*:* *:*:*
mouseNP_062722 HRNSIKFFTGDVFGYHG YTFANLG-EHEFVEEKT KVAKVSGVEDGPEAKRAKLD SSETTMVKKKVLFCPVKEAL 224
ratNP_001012063 HRNSIKFFTGDVFGYHG YTFANLG-EHEFVEEKT KVTKVSGVEDGPD AKRAKLD SSETTMVKKKVLFCPVKEAL 223
humanNP_005491.1 HKNSIKFFTGDVFGYHG YTFANLG-EHEFVEEKT KVAKVSGVEDGPD AKRAKLD SSETTMVKKKVVFCPVKEAL 220
zebrafishNP_001002058.1 ASRNKIVFCGDVYGYNG YMFSDLGOEYHYVEEKPKVVKGSNEANDGPEAKKPKIDPNETTMVKKKTI SFCSLKEAL 222

**:* **:*:* **:* ..***** ..**:* **:* **:* **:* **:* **:* **:* **:* **:* **:* **
mouseNP_062722 EVDWSGEKAKAALKRITAPDYFLLQVLLKFRIDKGRDPTSE SYKEDAELLQIRNDVFD SLGISP DLLPDDFVRYC 299
ratNP_001012063 AVDWSGEKAQAALKRITAPDYFLLQVLLKFRIDKGRDPTSDS YSEDAELLQIRNDVFD SLGISP DLLPDDFVRYC 298
humanNP_005491.1 EVDWSSEKAKAALKRITSDYFLLQVLLKFRIDKGRDPS SDTYEEDSELLQIRNDVLD SLGISP DLLPEDFVRYC 295
zebrafishNP_001002058.1 EVDWTEKAKSSLKRITAPDYFLLQVLLKFRIDKGRDPO PDSFAEDSOLLQIRDDVLETMGLS DLLPNTFVSYC 297

*****:*****:* ..***** ** ..*****:*.***:*.***:*.***:*.***:*.***:
mouseNP_062722 FSEMAPVCAVVG GILAQEIVKALSQRDPPHNNFFFDGMKGS GIVECLGPO 350
ratNP_001012063 FSEMAPVCAVVG GILAQEIVKALSQRDPPHNNFFFDGMKGS GIVECLGPO 349
humanNP_005491.1 FSEMAPVCAVVG GILAQEIVKALSQRDPPHNNFFFDGMKGN GIVECLGPK 346
zebrafishNP_001002058.1 FSEMSPCAVVG GVLGQEIVKALSQRDAPHRNFFFDGLKGS GVVDYFSSK 348

```

Fig. S2. Sae1 protein alignment in mouse, rat, human and zebrafish. The alignment was made by software ClustalX 2.0. The asterisk indicates 100% identical amino acids across four species. The C₈₁₇-to-T mutation resulted in production of a truncated Sae1 protein lacking the C-terminal 76 amino acids.

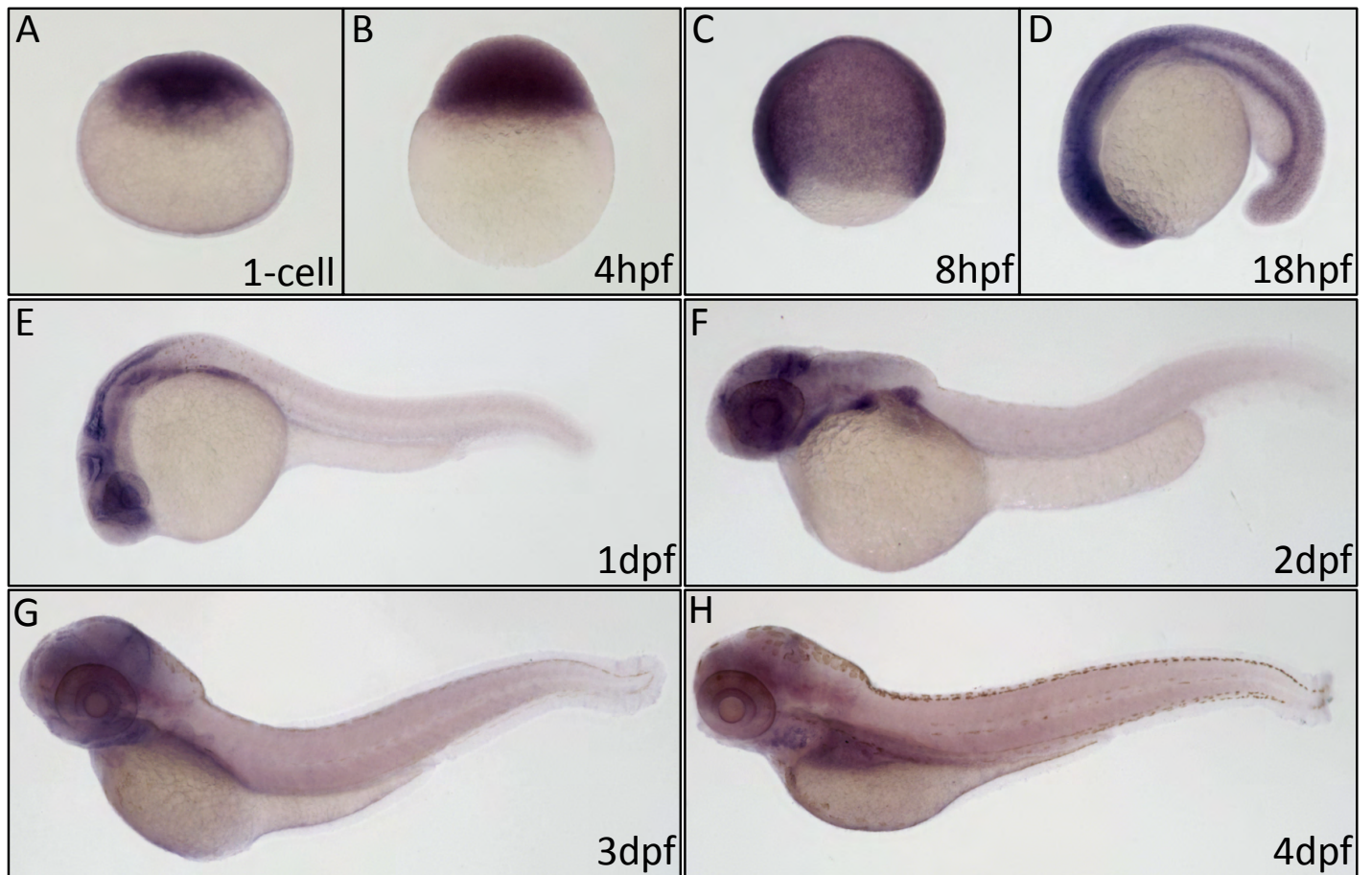


Fig. S3. The expression pattern of *sae1* during zebrafish early development. (A-H) WISH shows *sae1* expression in wild-type zebrafish at the 1-cell stage (A), 4 hpf (B), 8 hpf (C), 18 hpf (D), 1 dpf (E), 2 dpf (F), 3 dpf (G) and 4 dpf (H).

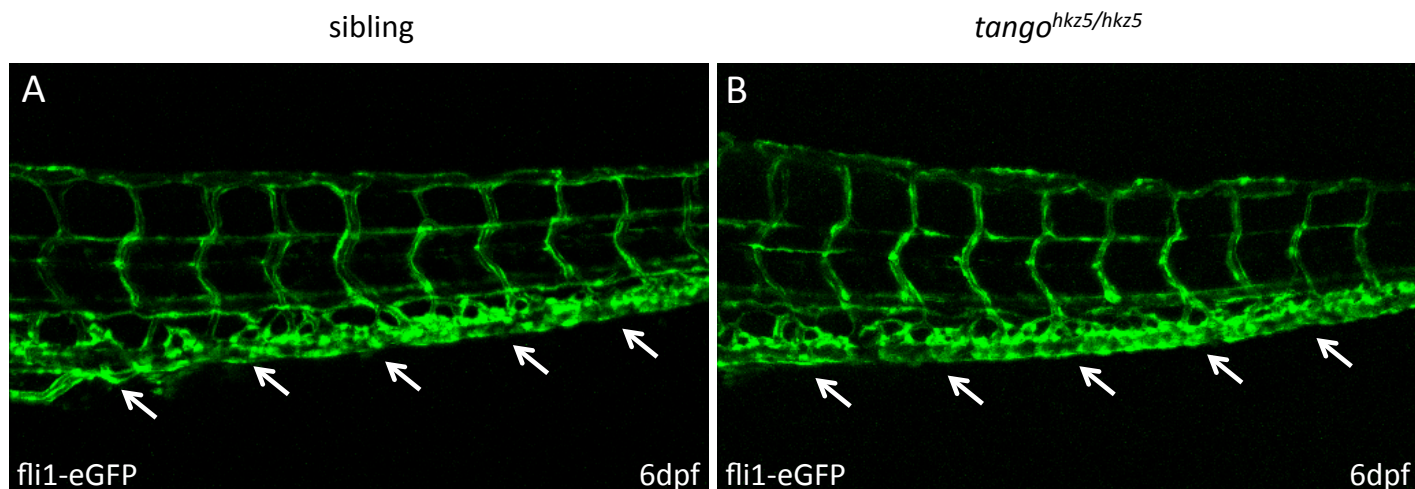


Fig. S4. The CHT vascular plexuses are intact in *tango*^{hkz5} mutants. (A,B) Anti-GFP staining reveals a similar overall structure of the CHT vascular plexuses (arrows) in the 6 dpf *Tg(fli1-eGFP)tango*^{hkz5/hkz5} mutants (B) and their siblings (A).

Table S1. Summary of chimera generation experiments (contribution to muscle and CNS)

Donor (dextran-injected fish)	Host (AB fish)	Total number of hosts	Number of hosts with dextran-labeled donor muscle cells in the trunk	Subgroup of donor-derived muscle cells			Percentage of dextran-labeled donor-derived muscle fibers* in the trunk muscle tissues	Number of hosts with dextran-labeled donor cells in the CNS
				<50 dextran-labeled cells	50-100 dextran-labeled cells	>100 dextran-labeled cells		
Sibling	Wild type	127	68 (53.5%)	19	19	30	0.4-6.3%	71 (55.9%)
<i>tango</i> ^{hkz5/hkz5}	Wild type	39	21 (53.8%)	5	5	11	0.2-5.9%	22 (56.4%)

*The total number of trunk muscle fibers in 5 dpf wild-type fish is estimated to be ~5000.